

Fundamental Limits on QBER and Distance in Quantum Key Distribution

Stefano Pirandola

Department of Computer Science, University of York, York YO10 5GH, United Kingdom

Quantum key distribution (QKD) enables information-theoretic secure communication, yet its ultimate tolerance to noise and achievable transmission distance remain fundamentally constrained. We establish the maximum quantum bit error rate (QBER) compatible with secure QKD and derive corresponding upper bounds on communication distance. Our results follow from a fundamental capacity threshold for qubit Pauli channels and apply to protocols based on two or more mutually unbiased bases, using either single-photon or weak coherent sources. By connecting information-theoretic limits to realistic physical noise models, we obtain universal bounds on achievable distances in fiber and free-space links, including diffraction-limited constraints relevant to deep-space quantum communications. These findings clarify the ultimate noise robustness of QKD and delineate the fundamental boundaries of secure quantum communication.

I. INTRODUCTION

Quantum key distribution (QKD) [1–3] is one of the most mature quantum technologies, currently being deployed in both research and industrial settings. Yet, QKD is affected by fundamental rate-loss limitations [4, 5] which require the use of intermediate repeater stations to form chains or networks of nodes, which may be trusted or untrusted [6–12]. The Pirandola-Laurenza-Ottaviani-Banchi (PLOB) bound [5] establishes that $-\log_2(1-\eta)$ is the maximum possible number of key bits per channel use that can be extracted over a lossy channel with transmissivity η . While this provides the maximum key rate achievable in repeaterless QKD, it does not directly impose a bound on the maximum quantum bit error rate (QBER) that is tolerable by discrete-variable (DV) protocols. This is the main result of this paper.

We begin by establishing a necessary and sufficient condition under which all two-way assisted capacities of the qubit Pauli channel are strictly positive. Building on this result, we then derive the threshold QBER values required to guarantee the security of a DV-QKD protocol employing either two or three mutually unbiased bases (MUBs). Next, we adopt a standard noise model that relates the QBER to the channel transmissivity and other relevant system parameters. Exploiting this relationship, we translate the QBER threshold conditions into bounds on the maximum transmission distance achievable by DV-QKD protocols over fiber-based and free-space links. Finally, we extend our analysis from the repeaterless setting to repeater-assisted protocols.

Our investigation not only establishes the fundamental limits of noise robustness for DV-QKD, but also reveals gaps in the existing literature. In particular, we identify the possibility of undiscovered DV-QKD protocols capable of tolerating higher QBERs than those currently known. Furthermore, we show that diffraction-limited free-space implementations can achieve exceptionally long transmission distances, thereby supporting the feasibility of deep-space quantum communications.

II. QUANTUM CHANNELS IN DV-QKD

In DV-QKD protocols, such as the BB84 protocol [1], there are two quantum channels involved, one affecting the system carrier (e.g., a photon or a photon pulse) and the other affecting the degree of freedom that is used for encoding and decoding (e.g., the polarization qubit). The first quantum channel is a bosonic lossy channel that transmits photons with probability η , referred to as the channel transmissivity. The second channel is a qubit Pauli channel. The lossy channel determines the detection rate, while the Pauli channel sets the QBER. Together, they determine the final secret key rate.

A qubit Pauli channel \mathcal{P} acts on a state ρ as follows

$$\mathcal{P}(\rho) = \sum_{k=0}^3 p_k P_k \rho P_k^\dagger, \quad (1)$$

where $\mathbf{p} := \{p_k\}$ is a probability distribution associated with the Pauli operators $P_k \in \{I, X, Y, Z\}$. Explicitly,

$$X = \begin{pmatrix} 0 & 1 \\ 1 & 0 \end{pmatrix}, \quad Y = \begin{pmatrix} 0 & -i \\ i & 0 \end{pmatrix}, \quad Z = \begin{pmatrix} 1 & 0 \\ 0 & -1 \end{pmatrix}, \quad (2)$$

with I being the 2×2 identity matrix.

The Pauli error probabilities can be connected with the values of the QBERs in the encoding bases. If the security of the QKD protocol is based on two MUBs, such as X and Z of the BB84 protocol, we have that the corresponding QBERs, known as bit error rate E_X and phase error rate E_Z , satisfy

$$E_X = p_2 + p_3, \quad E_Z = p_1 + p_2. \quad (3)$$

If the security of the QKD protocol is based on three MUBs, X , Z and Y , as in the six-state protocol [2], then the associated QBERs satisfy Eq. (3) and the additional relation $E_Y = p_1 + p_3$.

There are some relevant specific examples of Pauli channels. One is the bit-and-phase-flip (BPF) channel corresponding to the case with $p_2 = 0$. Since this channel only induces X and Z errors, it is the simplest model

compatible with QKD protocols based on two MUBs. Another relevant channel is the depolarizing one, which is a Pauli channel with equal errors in the three bases. This is typically parametrized as follows

$$\mathbf{p} = \left\{ 1 - \frac{3p}{4}, \frac{p}{4}, \frac{p}{4}, \frac{p}{4} \right\}, \quad (4)$$

and its action on a qubit state ρ reduces to the following

$$\mathcal{P}_{\text{depol}}(\rho) = (1-p)\rho + p\frac{I}{2}. \quad (5)$$

III. CAPACITY THRESHOLDS

Ref. [5] established the ultimate rates for entanglement distribution, quantum information transmission, and QKD in the absence of an intermediate relay. For specific channels, such as the bosonic lossy channel, the bosonic quantum-limited amplifier, and the dephasing and erasure channels, Ref. [5] derived the exact analytical expressions of the two-way assisted entanglement distribution capacity D_2 , the two-way assisted quantum capacity Q_2 , and the two-way assisted secret-key capacity K_2 , showing that these capacities coincide for these channels. Ref. [5] also provided lower and upper bounds for the two-way assisted capacities of the Pauli channel, the amplitude-damping channel and the thermal-loss channel. The latter channel was studied in several other papers, where the lower bound was improved [13–17].

Let us call \mathcal{C}_2 the generic two-way assisted capacity. Depending on the context, this can be D_2 , Q_2 or K_2 . As a direct consequence of Ref. [5], one obtains equivalent criteria for a quantum channel to satisfy $\mathcal{C}_2 = 0$. For a qubit Pauli channel, we show that

$$\mathcal{C}_2(\mathcal{P}) = 0 \iff p_{\max} := \max\{p_k\} \leq \frac{1}{2}, \quad (6)$$

and, for a depolarizing channel, we therefore have

$$\mathcal{C}_2(\mathcal{P}_{\text{depol}}) = 0 \iff p \geq \frac{2}{3}. \quad (7)$$

The proof in Appendix A relies on the fact that the two-qubit Choi state of a qubit Pauli channel has non-positive partial transposition (NPT) [18–22]. Note that this simple proof cannot be extended to higher dimensions since, already for qutrits (3×3), there is bound entanglement.

IV. MAXIMUM TOLERABLE QBER

We now exploit Eq. (6) to establish the maximum tolerable QBER in repeaterless QKD. Let us start by considering QKD protocols that are based on two MUBs, with observed QBERs E_X and E_Z . As the values of these QBERs gradually increase, the probability of the identity Pauli ‘error’ $p_0 = 1 - (E_X + E_Z) + p_2$ gradually decreases. Also, because the values of the QBERs

increase from zero, we have that $p_0 = p_{\max}$. According to Eq. (6), we find that QKD is possible as long as $E_X + E_Z < 1/2 + p_2$. In the worst-case scenario, Eve does not introduce Y errors ($p_2 = 0$), so we have a BPF channel and the maximum QBER is bounded as follows

$$E_X + E_Z < 1/2. \quad (8)$$

If this inequality is satisfied, then there certainly exists a QKD protocol with a positive key rate. If this is violated, the key rate is certainly zero for any QKD protocol.

Assuming the symmetric condition $E_X = E_Z := E$, we see that Eq. (8) becomes $E < 1/4$. It is interesting to note that this threshold coincides with the QBER induced by an intercept-resend attack against the BB84 protocol. While it may be intuitive to understand that security is not possible above $1/4$, it is less obvious to recognize that a QKD protocol (with suitable data processing) exists with a positive key rate up to $E = 1/4$. Previous studies [23] have identified that BB84 can be made secure up to $E = 18.9\%$ with suitable two-way data processing. Thus, our result raises the question of identifying a more powerful mechanism (protocol and/or data processing) able to effectively outperform $E = 18.9\%$ and approach the $1/4$ limit in the symmetric scenario.

Now consider QKD protocols based on three MUBs, with observed QBERs E_X , E_Z and E_Y . In this case, we repeat the previous reasoning to obtain $p_{\max} = p_0 = 1 - (E_X + E_Z + E_Y)/2$. Therefore, Eq. (6) leads to

$$E_X + E_Z + E_Y < 1. \quad (9)$$

Assuming symmetry $E_X = E_Z = E_Y := E$, we have $E < 1/3$. No QKD protocol based on three MUBs can be secure above this value in symmetric conditions. In fact, one can show that this corresponds to the threshold for an intercept-resend attack. As before, the less obvious point is that this result guarantees the existence of a QKD protocol based on three MUBs able to achieve a positive key rate up to $E = 1/3$. We know that the six-state protocol combined with two-way processing can achieve a QBER of 26.4% [23]. So it is another open question to discover the more powerful 3-MUB protocol (and/or data processing method) able to reach $1/3$.

V. NOISE MODEL FOR QBER IN DV-QKD

The QBER of a QKD protocol can be related to the total transmissivity η of the lossy channel connecting Alice and Bob. This relation allows one to translate the maximum tolerable QBER into a maximum achievable transmission distance. The exact translation depends on the noise model valid for the QBER, as we discuss below.

Consider the QBER E associated with a generic MUB (X , Z or Y). We can write the minimum value of E compatible with the transmissivity η and the relevant parameters of Alice’s source and Bob’s detectors. This ‘irreducible’ QBER represents the inevitable error rate

arising from loss and device imperfections, and therefore lower-bounds any observed QBER. Within the standard adversarial framework of QKD, all such noise is conservatively attributed to Eve and must be treated as channel noise associated with her perturbation of the systems.

Assume that Bob's detector has dark count probability Y_0 and misalignment error probability e_{det} , then the irreducible QBER has the form

$$E = \frac{\gamma e_{\text{det}} + (1 - \gamma)Y_0/2}{\gamma + (1 - \gamma)Y_0}, \quad (10)$$

where the analytical form of $\gamma = \gamma(\eta)$ depends on Alice's source. For a k -photon source, we may write $\gamma(\eta) = 1 - (1 - \eta)^k$, while for an attenuated coherent-state source with intensity μ , we have $\gamma(\eta) = 1 - e^{-\eta\mu}$.

For a decoy-state QKD protocol [24–30] with intensities μ_i and corresponding probabilities q_i , we can identify the intensity $\mu \in \{\mu_i\}$ associated with the best-case QBER. This QBER takes the form E_μ given by the right-hand-side of Eq. (10) with $\gamma(\eta) = 1 - e^{-\eta\mu}$. Then, the overall QBER of the protocol E is lower-bounded by E_μ . See Appendix B for more details on the QBER modelling.

VI. MAXIMUM DISTANCE

By combining the noise models of the previous section with the results on the maximum QBERs, we can bound the maximum distance achievable by QKD protocols under various assumptions. We consider the symmetric scenario where the QBERs associated with the different MUBs are equal to some common value E . This assumption can always be seen as a best-case scenario. In fact, if the QBERs differ, we can take their minimum $E = \min\{E_Z, E_X, \dots\}$ as a common value, thereby resulting in an upper bound on the maximum distance. Thus, our next results will provide distances beyond which QKD protocols are certainly not secure.

For a 2-MUB protocol, we can combine Eq. (10) with the symmetric threshold $E < 1/4$ to get the bound

$$\gamma(\eta) > \Gamma_2 := \frac{Y_0}{1 + Y_0 - 4e_{\text{det}}} \simeq Y_0. \quad (11)$$

Then, for a 3-MUB protocol, the previous formula in Eq. (11) is slightly modified into the following

$$\gamma(\eta) > \Gamma_3 := \frac{Y_0}{2 + Y_0 - 6e_{\text{det}}} \simeq Y_0/2. \quad (12)$$

Let us set $\Gamma = \Gamma_2$ or Γ_3 depending if we consider 2- or 3-MUB protocols. Then, for a single-photon implementation ($\gamma = \eta$), the bounds can compactly be written as $\eta > \Gamma$. For a practical implementation with an attenuated source of intensity μ (or a decoy-state implementation with best-case intensity μ), we instead have

$$\eta > -\frac{1}{\mu} \ln(1 - \Gamma). \quad (13)$$

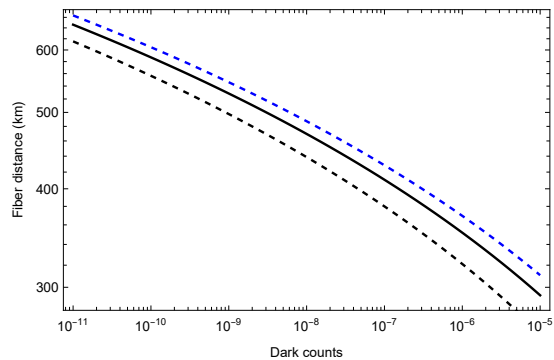


FIG. 1. Maximum fiber-distance in km versus dark count probability for a 2-MUB protocol with a single-photon source (solid black line), an attenuated source with intensity $\mu = 0.3$ (dashed black line) and intensity $\mu = 2$ (dashed blue line). We assume $\alpha = 0.17$ dB/km and $e_{\text{det}} = 1\%$.

The previous lower bounds for the transmissivity η can be written in terms of upper bounds for the distance d between Alice and Bob. First, we notice that we may decompose $\eta = \eta_{\text{eff}}\eta_{\text{ch}}$, where η_{eff} is the setup efficiency, i.e., the product of the transmissivities of Alice's and Bob's setups, while η_{ch} is the actual channel transmissivity, depending on the distance. In a fiber-based implementation, the fiber distance d can be computed assuming a loss-rate α in dB/km, using $\eta_{\text{ch}}(d) = 10^{-\alpha d/10}$. Therefore, by using $\gamma = \gamma[\eta_{\text{eff}}\eta_{\text{ch}}(d)]$ in Eqs. (11) or (12), we can bound the maximum distance achievable in fiber by repeaterless DV-QKD protocols. We may write

$$d < -\frac{10}{\alpha} \log_{10} \Omega, \quad \Omega := \begin{cases} \Gamma/\eta_{\text{eff}} & \text{1-photon,} \\ -\frac{\ln(1-\Gamma)}{\eta_{\text{eff}}\mu} & \text{attenuated.} \end{cases} \quad (14)$$

We can now derive numerical results. We assume perfect efficiency $\eta_{\text{eff}} = 1$, low-loss fiber $\alpha = 0.17$ dB/km, low dark counts 10^{-8} (compatible with SNSPD detectors) and low misalignment error $e_{\text{det}} = 1\%$. We find the results in Table I, which represent distances beyond which no key can be extracted. We can appreciate that the current distance records for repeaterless QKD experiments are not far from these values [31].

2-MUB		3-MUB	
1 photon	$\mu = 0.3$	1 photon	$\mu = 0.3$
470 km	439 km	488 km	457 km

TABLE I. Examples of maximum fiber-distance for various protocols (see text for the parameters used).

It is interesting to note how the maximum distance depends on the dark counts, as shown in Fig. 1. Because $Y_0 \ll 1$, we have the approximations in Eqs. (11) or (12). For single-photon protocols, this means $d \simeq -\log_{10} Y_0$.

VII. MAXIMUM FREE-SPACE DISTANCE

In free space, optical links are more generally described as fading channels, since pointing errors and large-scale turbulence induce random beam wandering across the receiver aperture [32–34]. For our upper bound, we ignore the fading process and consider the maximum transmissivity of the free-space link. Its value is determined by diffraction, small-scale turbulence, and atmospheric absorption. In general, we may decompose $\eta_{\text{ch}} = \eta_{\text{fs}}\eta_{\text{atm}}$.

On the ground, the atmospheric component can be modelled by the Beer-Lambert extinction equation

$$\eta_{\text{atm}}(d) = \exp[-\alpha(h)d], \quad (15)$$

where d is the horizontal path length in the atmosphere, and $\alpha(h)$ is the extinction factor at the altitude h [35–37]. A good approximation valid for the optical wavelength of $\lambda = 800$ nm at near sea-level is $\alpha(h) = \alpha_0 \exp(-h/H)$, where $\alpha_0 \simeq 5 \times 10^{-3} \text{ km}^{-1}$ and $H = 6.6 \text{ km}$ [32, 38]. For a satellite link, the atmospheric extinction varies with the altitude. For a satellite at slant distance $d = d(h, \theta)$, where h is the altitude and $\theta \leq 1$ is the zenith angle, we can write $\eta_{\text{atm}}(d) \simeq [\eta_{\text{atm}}^{\text{zen}}(h)]^{\sec(\theta)}$, where $\eta_{\text{atm}}^{\text{zen}}$ is the transmissivity at the zenith position. For $h > 30 \text{ km}$, we can approximate $\eta_{\text{atm}}^{\text{zen}} \simeq 0.967$ at $\lambda = 800 \text{ nm}$ [33].

The free-space component η_{fs} is associated with beam waist broadening induced by diffraction and small-scale turbulence (inner-scale turbulence effects). Approximate analytical formulas can be written for weak and strong regimes of turbulence, while the intermediate behaviour can only be explored numerically [39, 40]. Starting from the adopted turbulence model, one can write or numerically evaluate the spot size of the beam at distance d and compute $\eta_{\text{fs}}(d)$. Then, by using $\gamma = \gamma[\eta_{\text{eff}}\eta_{\text{fs}}(d)\eta_{\text{atm}}(d)]$ in Eqs. (11) or (12), we can bound the maximum distance for free-space QKD, which can be applied to ground-based or ground-satellite implementations.

Here, we derive a universal upper bound which ignores turbulence and only considers the effect induced by diffraction. This bound applies to all free-space implementations, but it is specifically meaningful for deep-space communications where the atmospheric effects can be completely ignored. This diffraction-limited bound can be derived by using $\eta_{\text{atm}}(d) \leq 1$ and

$$\eta_{\text{fs}}(d) \leq \eta_{\text{diff}}(d) = 1 - e^{-2a_R^2/w_d^2} \simeq \frac{2a_R^2}{w_d^2}. \quad (16)$$

Here a_R is the radius of the receiver circular aperture, and w_d is the beam spot size at distance d , given by

$$w_d^2 = w_0^2 \left[(1 - d/R_0)^2 + (d/d_R)^2 \right] \geq w_0^2 (d/d_R)^2, \quad (17)$$

where w_0 is the field spot size of the Gaussian beam generated by Alice, with carrier wavelength λ and curvature R_0 , while $d_R := \pi w_0^2 \lambda^{-1}$ is the Rayleigh range [41–44]. In this way, we get the following diffraction-limited upper

bound for the maximum QKD distance

$$d < \frac{\pi w_0 a_R}{\lambda} \sqrt{\frac{2}{\Omega'}}, \quad \Omega' := -\ln(1 - \Omega) \simeq \Omega, \quad (18)$$

where Ω takes the expressions in Eq. (14), depending on the use of single-photon or attenuated QKD sources.

Let us investigate the limits of deep-space QKD, assuming $\eta_{\text{eff}} = 1$, $Y_0 = 10^{-8}$ and $e_{\text{det}} = 1\%$ as before. Then, we consider Alice sending a collimated Gaussian beam of initial waist $w_0 = 2 \text{ m}$ at $\lambda = 800 \text{ nm}$, and Bob receiving it with a telescope of radius $a_R = 0.5 \text{ m}$. If we adopt a 3-MUB protocol with a single-photon source, we get $d < 7.73 \times 10^7 \text{ km}$, which is an interplanetary distance, on the order of the Earth–Mars distance at a relatively close approach. Of course, this would be an absolute upper bound, not accounting for practical imperfections such as pointing errors, etc.

VIII. REPEATER-BASED PROTOCOLS

In order to extend the results to repeater-based protocols, we can leverage Ref. [45]. Let us assume that Alice and Bob are connected by N repeaters, so we have $N + 1$ links. Each link i induces a lossy channel and a Pauli channel \mathcal{P}_i . For each \mathcal{P}_i with probabilities $\{p_k^i\}$, we consider $p_{\text{max}}^i = \max p_k^i$. For the entire sequence of Pauli channels $\{\mathcal{P}_i\}$, we take the bottleneck value $p_{\text{max}}^{\text{min}} := \min_i p_{\text{max}}^i$. As briefly explained in Appendix C, the end-to-end two-way assisted capacity of the repeater chain $\mathcal{C}_2(\{\mathcal{P}_i\})$ satisfies

$$p_{\text{max}}^{\text{min}} \leq 1/2 \implies \mathcal{C}_2(\{\mathcal{P}_i\}) = 0. \quad (19)$$

As before, this condition can be translated into a threshold for the maximum QBER. If each link on the chain implements a 2-MUB protocol with QBERs E_Z^i and E_X^i , we must have

$$\max_i \{E_X^i + E_Z^i\} < 1/2. \quad (20)$$

If this threshold is violated, then no key rate can be extracted. However, since the converse implication in Eq. (19) does not hold, we cannot assert the existence of a repeater-based protocol that achieves a positive key rate when the total QBER approaches 1/2. An analogous situation arises if the chain implements 3-MUB protocols, in which case the corresponding bound would be written as $\max_i \{E_X^i + E_Z^i + E_Y^i\} < 1$.

Finally, these results admit a straightforward interpretation in terms of maximum transmission distance. In particular, the distance constraint identified for the repeaterless configuration also governs the longest individual segment within a repeater chain.

IX. CONCLUSIONS

In this work, we established the maximum tolerable QBER for DV-QKD protocols and bounded their max-

imum distance in both fiber-based and free-space implementations. We considered protocols based on two or more MUBs, and whose implementation employs either single-photon or weak coherent (attenuated) sources. While we derived the main results for the repeaterless configuration, we also showed that their extension to the repeater-based setting is immediate.

Our results imply the existence of undiscovered QKD protocols and/or data processing methods that are able to overcome the best performance known so far. Identifying such protocols and/or methods is left as an open question for the community. In the free-space scenario, we showed that geometric diffraction imposes a fundamental upper bound on the maximum transmission distance; nevertheless, this limit remains sufficiently large to enable long-range implementations, including deep-space quantum communications.

ACKNOWLEDGMENTS

This work was supported by the Integrated Quantum Networks (IQN) Research Hub (EPSRC, Grant No. EP/Z533208/1).

Appendix A: Zero-capacity thresholds

This is a simple proof of Eq. (6) of the main text. First observe that the two-way assisted capacity of a Pauli channel \mathcal{P} with probabilities $\{p_k\}$ satisfies [5]

$$\mathcal{C}_2(\mathcal{P}) \leq \Phi(\mathcal{P}) := \begin{cases} 1 - H_2(p_{\max}), & p_{\max} \geq \frac{1}{2}, \\ 0, & \text{otherwise,} \end{cases} \quad (\text{A1})$$

where H_2 is the binary Shannon entropy computed on $p_{\max} = \max\{p_k\}$. From Eq. (A1), we see that $p_{\max} \leq \frac{1}{2}$ implies $\mathcal{C}_2(\mathcal{P}) = 0$. Then we ask if $\mathcal{C}_2(\mathcal{P}) = 0$ implies $p_{\max} \leq \frac{1}{2}$, so we can write an equivalence.

A basic strategy for distributing entanglement over a Pauli channel \mathcal{P} is to send half of a Bell state through the channel. Alice keeps one qubit and sends the other qubit to Bob. After the channel, the joint two-qubit output is the Choi state of the qubit Pauli channel. This is a Bell-diagonal state with spectral decomposition

$$\rho_{\mathcal{P}} = \sum_{k=0}^3 p_k \Phi_k, \quad (\text{A2})$$

where the eigenvalues coincide with the channel probabilities and $\{\Phi_k\}$ are the four Bell states.

It is immediate to check that the two-qubit Choi state $\rho_{\mathcal{P}}$ in Eq. (A2) is an NPT state [18, 19] for $p_{\max} > 1/2$. Because, in dimensions 2×2 , all NPT states have non-zero distillable entanglement [20–22], we have that $\rho_{\mathcal{P}}$ has non-zero distillable entanglement $E_D(\rho_{\mathcal{P}}) > 0$. Thus, this basic strategy for entanglement distribution guarantees that entanglement can be distilled from the output

state of the Pauli channel if we have $p_{\max} > 1/2$. This means that $p_{\max} > 1/2$, implies $\mathcal{C}_2(\mathcal{P}) \geq E_D(\rho_{\mathcal{P}}) > 0$ or, equivalently, that $\mathcal{C}_2(\mathcal{P}) = 0$ implies $p_{\max} \leq 1/2$.

Finally, because the depolarizing channel is a Pauli channel with probabilities as in Eq. (4) of the main text, we automatically derive Eq. (7) of the main text.

Appendix B: QBER noise modelling

Let us write the details of relevant formulas here. Assume that Alice sends a k -photon state through a lossy channel with transmissivity η , and Bob has a threshold detector at its output, which is the standard case in DV-QKD. Then, the transmissivity of a k -photon signal is

$$\eta_k = 1 - (1 - \eta)^k, \quad (\text{B1})$$

so that $\eta_0 = 0$, $\eta_1 = \eta$, etc. This is the probability that at least one photon passes the threshold detector [28].

Given an input k -photon state, we adopt the union model in which a detection event occurs either due to a signal click or due to a dark count in the absence of a signal click. For this reason, the yield takes the form

$$Y_k = \eta_k + (1 - \eta_k)Y_0, \quad (\text{B2})$$

where Y_0 is the dark count probability. Correspondingly, we also consider the error yield, i.e., the overall probability of an erroneous detection. This is given by

$$P_k = e_{\text{det}}\eta_k + (1 - \eta_k)Y_0/2, \quad (\text{B3})$$

where e_{det} is the misalignment error associated with signal clicks. Thus, the minimum QBER reads

$$E_k = \frac{P_k}{Y_k} \simeq \frac{e_{\text{det}}\eta_k + Y_0/2}{\eta_k + Y_0}. \quad (\text{B4})$$

In particular, if Alice has an ideal single-photon source, then the QBER is given by Eq. (B4) for $k = 1$.

In practical QKD implementations, Alice has an attenuated coherent-state source with mean number of photons (intensity) μ , which generates k -photon signals according to a Poisson distribution $p_A^\mu(k) = (\mu^k/k!)e^{-\mu}$. For the intensity μ , we consider the gain Q_μ , which is the overall probability of a detection event, and the error gain P_μ , which is the overall probability of an error [28]. These are given by

$$P_\mu = e_{\text{det}}(1 - e^{-\eta\mu}) + e^{-\eta\mu}Y_0/2, \quad (\text{B5})$$

$$Q_\mu = 1 - e^{-\eta\mu} + e^{-\eta\mu}Y_0. \quad (\text{B6})$$

The QBER associated with the intensity μ is

$$E_\mu = \frac{P_\mu}{Q_\mu} \simeq \frac{e_{\text{det}}(1 - e^{-\eta\mu}) + Y_0/2}{1 - e^{-\eta\mu} + Y_0}. \quad (\text{B7})$$

In the case of decoy-state protocols, Alice randomly chooses between various intensities $\mu_i \geq 0$ with probabilities $q_i > 0$. The expected minimum QBER can be

written as

$$E = \frac{\sum_i c_i q_i P_{\mu_i}}{\sum_i c_i q_i Q_{\mu_i}}, \quad (\text{B8})$$

where $c_i = [1 + r_s Q_{\mu_i} \tau_{\text{dt}}]^{-1}$ is a factor depending on the repetition rate of Alice's source r_s and the dead time τ_{dt} of Bob's detector [29, 30].

Setting $E_{\mu_i} = P_{\mu_i}/Q_{\mu_i}$, it is easy to check that

$$\min_i \{E_{\mu_i}\} \leq E \leq \max_i \{E_{\mu_i}\} \leq \sum_i E_{\mu_i}. \quad (\text{B9})$$

In fact, we can assume $Q_{\mu_i} > 0$ for all i , and write

$$E = \sum_i \lambda_i E_{\mu_i}, \quad (\text{B10})$$

where

$$\lambda_i := \frac{c_i q_i Q_{\mu_i}}{\sum_j c_j q_j Q_{\mu_j}}, \quad \lambda_i > 0, \quad \sum_i \lambda_i = 1. \quad (\text{B11})$$

Because E is convex in E_{μ_i} , we have Eq. (B9).

As a result, we can choose $i^* = \arg \min_i E_{\mu_i}$ and consider $E_{\mu_{i^*}}$ as the minimum achievable QBER. This is equivalent to use E_{μ} in Eq. (B7) where we set $\mu = \mu_{i^*}$. In our study, we therefore use Eq. (B7) as the minimum achievable QBER for decoy-based QKD implementations. It is understood that this provides a best-case scenario, so that using this modelling will provide an upper bound for the maximum distance.

Appendix C: Zero-capacity thresholds for repeater chains

For a qubit Pauli channel, the upper bound $\Phi(\mathcal{P})$ in Eq. (A1) comes from the relative entropy of entanglement E_R (REE) [46, 47] computed over its Choi state $\sigma_{\mathcal{P}}$. If we have a chain of N intermediate repeaters between Alice and Bob, we have a total of $N + 1$ Pauli channels \mathcal{P}_i on the chain. According to Ref. [45, Th. 3], we have that the end-to-end capacity between Alice and Bob satisfies

$$\mathcal{C}_2(\{\mathcal{P}_i\}) \leq \min_i E_R(\sigma_{\mathcal{P}_i}) = \min_i \Phi(\mathcal{P}_i). \quad (\text{C1})$$

For channel \mathcal{P}_i with probabilities $\{p_k^i\}$, let us define $p_{\text{max}}^i := \max_k \{p_k^i\}$. Then, we take the minimum along the chain $p_{\text{max}}^{\min} := \min_i p_{\text{max}}^i$, and we can write

$$\mathcal{C}_2(\{\mathcal{P}_i\}) \leq \begin{cases} 1 - H_2(p_{\text{max}}^{\min}), & p_{\text{max}}^{\min} \geq \frac{1}{2}, \\ 0, & \text{otherwise.} \end{cases} \quad (\text{C2})$$

This result means that $p_{\text{max}}^{\min} \leq 1/2$ certainly implies $\mathcal{C}_2(\{\mathcal{P}_i\}) = 0$. Unfortunately, the opposite cannot be proven using the simple approach of the repeaterless case. The problem is that the Bell detections performed at the repeaters (necessary to extend entanglement to the end points) will gradually decrease the fidelity if the states distributed over the links are not perfect Bell pairs.

-
- [1] C. H. Bennett and G. Brassard, "Quantum cryptography: Public key distribution and coin tossing," Proceedings of IEEE International Conference on Computers, Systems and Signal Processing, Bangalore, India, pp. 175–179 (1984).
- [2] D. Bruss, "Optimal Eavesdropping in Quantum Cryptography with Six States," Phys. Rev. Lett. **81**, 3018 (1998)
- [3] S. Pirandola, U. L. Andersen, L. Banchi, M. Berta, D. Bunandar, R. Colbeck, D. Englund, T. Gehring, C. Lupo, C. Ottaviani, et al., "Advances in quantum cryptography," Advances in Optics and Photonics **12**, 1012 (2020).
- [4] S. Pirandola, R. Garcia-Patron, S. L. Braunstein, and S. Lloyd, "Direct and Reverse Secret-Key Capacities of a Quantum Channel," Phys. Rev. Lett. **102**, 050503 (2009).
- [5] S. Pirandola, R. Laurenza, C. Ottaviani and L. Banchi, "Fundamental Limits of Repeaterless Quantum Communications," Nature Comm. **8**, 15043 (2017)
- [6] S. L. Braunstein and S. Pirandola, "Side-Channel-Free Quantum Key Distribution," Phys. Rev. Lett. **108**, 130502 (2012).
- [7] H.-K. Lo, M. Curty, and B. Qi, "Measurement-Device-Independent Quantum Key Distribution," Phys. Rev. Lett. **108**, 130503 (2012).
- [8] M. Lucamarini, Z. L. Yuan, J. F. Dynes, and A. J. Shields, "Overcoming the rate-distance limit of quantum key distribution without quantum repeaters," Nature **557**, 400 (2018).
- [9] X.-B. Wang, Z.-W. Yu, and X.-L. Hu, "Twin-field quantum key distribution with large misalignment error," Phys. Rev. A **98**, 062323 (2018).
- [10] Z.-W. Yu, X.-L. Hu, C. Jiang, H. Xu and X.-B. Wang, "Sending-or-not-sending twin-field quantum key distribution in practice," Sci. Rep. **9**, 3080 (2019).
- [11] C. Jiang, Z.-W. Yu, X.-L. Hu, and X.-B. Wang, "Unconditional security of sending or not sending twin-field quantum key distribution with finite pulses," Phys. Rev. Applied **12**, 024061 (2019).
- [12] C. Cui, Z.-Q. Yin, R. Wang, W. Chen, S. Wang, G.-C. Guo, and Z.-F. Han, "Twin-field Quantum Key Distribution without Phase Postselection," Phys. Rev. Applied **11**, 034053 (2019).
- [13] C. Ottaviani, R. Laurenza, T. P. W. Cope, G. Spedalieri, S. L. Braunstein, S. Pirandola, "Secret key capacity of the thermal-loss channel: improving the lower bound," SPIE proceedings Quantum Information Science and technology II, 9996, 999609 (2016).
- [14] S. Pirandola, S. L. Braunstein, R. Laurenza, C. Ottaviani, T. P. W. Cope, G. Spedalieri, and L. Banchi, "Theory of

- channel simulation and bounds for private communication,” *Quantum Sci. Technol.* **3**, 035009 (2018).
- [15] G. Wang, C. Ottaviani, H. Guo, S. Pirandola, “Improving the lower bound to the secret-key capacity of the thermal amplifier channel,” *Eur. Phys. J. D* **73**, 17 (2019).
- [16] F. A. Mele, L. Lami, and V. Giovannetti, “Maximum tolerable excess noise in continuous-variable quantum key distribution and improved lower bound on two-way capacities,” *Nature Photonics* **19**, 329 (2025).
- [17] G. Ortolano, S. Pirandola, and L. Banchi, “Lower Bounding the Secret Key Capacity of Bosonic Gaussian Channels via Optimal Gaussian Measurements,” arXiv:2512.15502 (2025).
- [18] A. Peres, “Separability Criterion for Density Matrices,” *Phys. Rev. Lett.* **77**, 1413 (1996).
- [19] M. Horodecki, P. Horodecki, R. Horodecki, “Separability of mixed states: necessary and sufficient conditions,” *Phys. Lett. A* **223**, 1 (1996).
- [20] M. Horodecki, P. Horodecki and R. Horodecki, “Density Matrices Can Be Distilled to a Singlet Form,” *Phys. Rev. Lett.* **78**, 574 (1997).
- [21] M. Horodecki, P. Horodecki, R. Horodecki, “Mixed-State Entanglement and Distillation: Is there a ‘Bound’ Entanglement in Nature?”, *Phys. Rev. Lett.* **80**, 5239 (1998).
- [22] R. Horodecki, “Distillation and bound entanglement,” *Phys. Rev. A* **60**, 1888 (1999).
- [23] D. Gottesman, and H.-K. Lo, “Proof of security of quantum key distribution with two-way classical communications,” *IEEE Trans. Inf. Theory* **49**, 457 (2003).
- [24] W.-Y. Hwang, “Quantum Key Distribution with High Loss: Toward Global Secure Communication,” *Phys. Rev. Lett.* **91**, 057901 (2003).
- [25] X.-B. Wang, “Beating the photon-number-splitting attack in practical quantum cryptography,” *Phys. Rev. Lett.* **94**, 230503 (2005).
- [26] X.-B. Wang, “Decoy-state protocol for quantum cryptography with four different intensities of coherent light,” *Phys. Rev. A* **72**, 012322 (2005).
- [27] H.-K. Lo, X. Ma, and K. Chen, “Decoy State Quantum Key Distribution,” *Phys. Rev. Lett.* **94**, 230504 (2005).
- [28] X. Ma, “Quantum cryptography: from theory to practice”, PhD Thesis (2008).
- [29] V. Burenkov, B. Qi, B. Fortescue, and H.-K. Lo, “Security of high speed quantum key distribution with finite detector dead time,” *Quantum Info. Comput.* **14**, 217 (2014).
- [30] D. Rusca, A. Boaron, F. Grünfelder, A. Martin, and H. Zbinden, “Finite-key analysis for the 1-decoy state QKD protocol,” *Appl. Phys. Lett.* **112**, 171104 (2018).
- [31] A. Boaron, G. Boso, D. Rusca, C. Vulliez, C. Autebert, M. Caloz, M. Perrenoud, G. Gras, F. Bussi eres, M.-J. Li, D. Nolan, A. Martin, and H. Zbinden, “Secure Quantum Key Distribution over 421 km of Optical Fiber,” *Phys. Rev. Lett.* **121**, 190502 (2018).
- [32] S. Pirandola, “Limits and Security of Free-Space Quantum Communications,” *Phys. Rev. Research* **3**, 013279 (2021).
- [33] S. Pirandola, “Satellite Quantum Communications: Fundamental Bounds and Practical Security”, *Phys. Rev. Research* **3**, 023130 (2021).
- [34] S. Pirandola, “Composable security for continuous variable quantum key distribution: Trust levels and practical key rates in wired and wireless networks”, *Phys. Rev. Research* **3**, 043014 (2021).
- [35] C. F. Bohren, and D. R. Huffman, “Absorption and scattering of light by small particles” (John Wiley & Sons, Inc., 2008).
- [36] H. Kaushal, V. K. Jain, and S. Kar, “Free Space Optical Communication” (Springer, New York, 2017).
- [37] S. Q. Duntley, “The reduction of apparent contrast by the atmosphere”, *J. Opt. Soc. Am.* **38**, 179 (1948).
- [38] D. Vasylyev, W. Vogel, and F. Moll, “Satellite-mediated quantum atmospheric links”, *Phys. Rev. A* **99**, 053830 (2019).
- [39] H. Yura, “Short term average optical-beam spread in a turbulent medium”, *J. Opt. Soc. Am.* **63**, 567-572 (1973).
- [40] R. L. Fante, “Electromagnetic Beam Propagation in Turbulent Media”, *Proc. IEEE* **63**, 1669 (1975).
- [41] A. Siegman, “Lasers” (University Science Books, 1986).
- [42] O. Svelto, “Principles of Lasers”, 5th edn. (Springer, New York 2010).
- [43] L. C. Andrews, W. B. Miller, and J. C. Ricklin, “Geometrical representation of Gaussian beams propagating through complex paraxial optical systems”, *Appl. Opt.* **32**, 5918-5929 (1993).
- [44] L. C. Andrews, W. B. Miller, and J. C. Ricklin, “Spatial coherence of a Gaussian-beam wave in weak and strong optical turbulence”, *J. Opt. Soc. Am. A* **11**, 1653-1660 (1994).
- [45] S. Pirandola, “End-to-end capacities of a quantum communication network”, *Commun Phys* **2**, 51 (2019).
- [46] V. Vedral, M. B. Plenio, M. A., Rippin, and P. L. Knight, “Quantifying Entanglement”, *Phys. Rev. Lett.* **78**, 2275 (1997).
- [47] V. Vedral, and M. B. Plenio, “Entanglement measures and purification procedures”, *Phys. Rev. A.* **57**, 1619 (1998).